

Limitations of delayed state feedback: a numerical study

Wim Michiels
Dirk Roose

Report TW 323, April 2001



Katholieke Universiteit Leuven
Department of Computer Science
Celestijnenlaan 200A – B-3001 Heverlee (Belgium)

Limitations of delayed state feedback: a numerical study

Wim Michiels

Dirk Roose

Report TW 323, April 2001

Department of Computer Science, K.U.Leuven

Abstract

In [8] a new numerical stabilization method for linear time-delay systems was proposed and applied to the stabilization of linear time-invariant systems with an input delay using static state feedback. In this paper we study the limitations of such delayed state feedback laws. More precisely we completely characterize the class of stabilizable plants in the 2D-case. Therefore we make use of numerical continuation techniques. The use of delayed state feedback in various control applications and the effect of its limitations are briefly discussed.

Keywords : delay equation, stability, numerical continuation

1 Introduction

Time-delays between input and output are common phenomena in industrial processes, engineering systems, economical and biological systems. They are e.g. introduced by transportation and communication lags, and also arise when distributed parameter systems are approximated by low-order models with delay [6, 7]. Time-delays generally have a destabilizing influence in a control loop and make the design of a satisfactory controller difficult to achieve. When delays are not taken into account, a severe degradation of performance and even instability may occur [10].

In [8] a new numerical stabilization method for linear time-delay systems, called the continuous pole placement method, was proposed, extending the classical pole placement algorithm for ODE models to a class of delay differential equations (DDEs). Unlike methods based on finite spectrum assignment (FSA), see [1, 13] and the references therein, this method does not render the closed loop system finite dimensional but consists of controlling the right most eigenvalues, which are moved to the left half plane in a quasi-continuous way by applying small changes to the controller parameters. The continuous pole placement method was illustrated in [8] by means of the stabilization of the linear controllable system,

$$\dot{x} = Ax + Bu(t - T), \quad A \in \mathbb{R}^{n \times n}, \quad B \in \mathbb{R}^{n \times 1}, \quad (1)$$

where $x \in \mathbb{R}^n$ is the state, $u \in \mathbb{R}$ is the input and $T \in \mathbb{R}^+$ represents an input delay. Using a linear static state feedback controller,

$$u = K^T x, \quad K \in \mathbb{R}^{n \times 1}, \quad (2)$$

the closed loop system (1)-(2) takes the form

$$\dot{x} = Ax + BK^T x(t - T), \quad (3)$$

and the continuous pole placement method allows to compute the feedback gain K .

In [8] some restrictions of delayed state feedback, i.e. the term $K^T x(t - T)$ in (3), were considered. For instance when the uncontrolled system (1) is unstable, it is generally not stabilizable with static state feedback for large delay values. On the other hand it was also indicated that stability, achieved with delayed state feedback, is robust w.r.t. small parameter changes and that the continuous pole placement method has stabilizability properties comparable to FSA methods when small parameter changes and implementation errors of the control law are taken into account. The latter are analysed for FSA methods in [2, 4].

In this paper we perform a thorough study of the stabilizability of the system (3) in the 2D-case. More precisely we characterize the class of systems (1) which are stabilizable with (delayed) state feedback. Therefore we make use of numerical tools as continuation and bifurcation analysis [11].

Note that equation (3) is of the form

$$\dot{x} = Ax + Mx(t - T), \quad (4)$$

where the feedback matrix $M = BK^T$ is of rank 1. We will also consider the case where all components of M can be chosen independently. This allows to extend the class of stabilizable systems considerably and forms however no restriction since we will show that when the problem with arbitrary M , (4), can be solved, it is always possible to construct a stabilizing controller for (1).

Although the stabilizability of (3)-(4) is a problem on its own, independent of practical numerical methods for calculating the feedback gain, we start in this paper from the continuous pole placement method, since its application reveals some important properties of the systems (3)-(4), which form the starting point of our stability analysis.

The structure of the paper is as follows. First we illustrate the continuous pole placement method [8] by means of a numerical example. Then we study the stability properties of (3)-(4) in the 2D case. Finally we briefly discuss some applications of delayed state feedback, including an extension of the classical Smith Predictor [10, 12] to a class of unstable systems.

2 Continuous pole placement method

The zero solution of the DDE (4) is asymptotically stable if all its eigenvalues, i.e. the roots of the characteristic equation,

$$\det \left(\lambda I - A - Me^{-\lambda T} \right) = 0, \quad (5)$$

are in the open left half plane [6]. When the control term $M \neq 0$, equation (5) is transcendental and has infinitely many solutions. A direct generalization of the pole placement algorithm is therefore not possible since the number of controller parameters in (3) and (4) is finite. However the number of eigenvalues of (4) to the right of any vertical line $\Re(\lambda) = r$ with $r \in \mathbb{R}$ is also finite, while $-\infty$ is the only accumulation point for the real parts of the eigenvalues [6]. In the continuous pole placement method, the controller parameters are used to control only the rightmost or unstable eigenvalues.

It consists of moving the rightmost eigenvalues of the DDE into the left half plane or to a desired location by applying small parameter changes and meanwhile monitoring the other eigenvalues with a large real part. The latter is possible with an algorithm to compute the rightmost eigenvalues of a DDE, for instance the algorithm described in [5], which is based on subspace iteration. Another algorithm, based on the discretisation of the semigroup operator associated with the DDE, is incorporated in the software package DDE-BIFTOOL [3].

In Figures 1–2 the continuous pole placement method is illustrated for the system (3), where

$$A = \begin{bmatrix} 1 & 0 \\ 1 & -1 \end{bmatrix}, \quad B = \begin{bmatrix} 1 \\ 0 \end{bmatrix}, \quad T = 1. \quad (6)$$

The controller gain K , shown in Figure 2, is continuously adapted in order to move the rightmost eigenvalues to the left half plane, see Figure 1. For $K = 0$, only the two eigenvalues of the open loop system occur. When $K \neq 0$, the number of eigenvalues is infinite. First the real part of only one eigenvalue is reduced, and from iteration number 100 on we control the two rightmost eigenvalues and are able to achieve stability. Around iteration step 215 the method breaks down, thereby reaching the global minimum of $\sup \Re(\lambda)$, where 3 real eigenvalues coincide. In the next section we will investigate properties of such extrema in detail.

3 Characterization of stabilizable systems

As illustrated in the previous section and noticed in [8], the closed loop eigenvalues cannot be moved arbitrarily far into the left half plane with delayed state feedback. Furthermore, when the uncontrolled system is unstable, it is not always possible to achieve stability. In [8], it was proven that in the scalar case, i.e. $\dot{x} = ax + m x(t-T)$, $x \in \mathbb{R}$, we have, $\inf_m \sup \Re(\lambda) = a - 1/T$, hence stabilization is only possible when $aT < 1$.

We now illustrate the limitations of delayed state feedback for the two-dimensional case. Consider therefore equation (4), with $A, M \in \mathbb{R}^{2 \times 2}$. We treat both cases where M is of rank 1, for instance $M = BK^T$ as in (3), and where the components of M can be chosen independently, and determine the class of stabilizable plants. For simplicity we first assume that the time-delay is equal to one. The case where $T \neq 1$ will be treated separately.

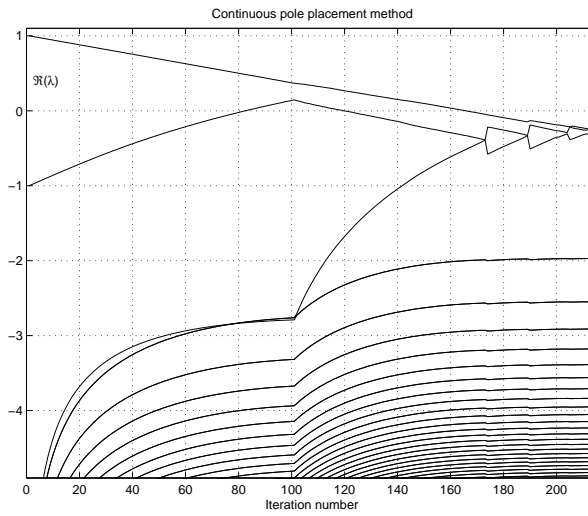


Figure 1: Real parts of the rightmost eigenvalues as a function of the iterations of the continuous pole placement algorithm. When no further reduction of $\sup \Re(\lambda)$ is possible, there are three coinciding rightmost eigenvalues.

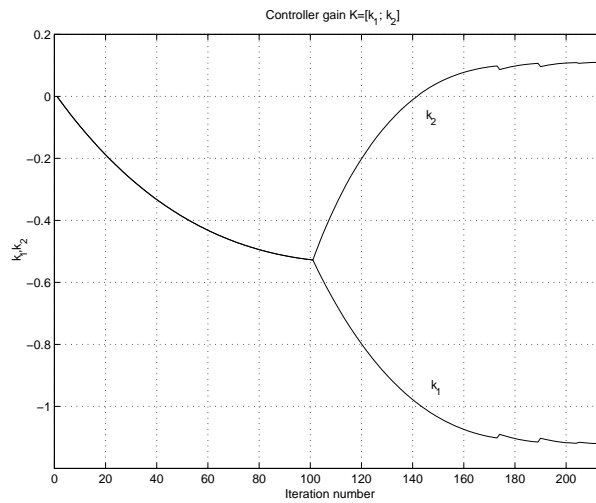


Figure 2: Controller gain, $K = [k_1 \ k_2]^T$, as a function of the number of iterations in the continuous pole placement algorithm.

3.1 System representation

In the 2-D case and for $T = 1$, system (4) can be transformed into the form

$$\dot{x} = \begin{bmatrix} 0 & 1 \\ -a_2 & -a_1 \end{bmatrix} x + \begin{bmatrix} -k_4 & -k_3 \\ -k_2 & -k_1 \end{bmatrix} x(t-1). \quad (7)$$

Furthermore when $M = BK^T$ as in (3), with the pair (A, B) controllable, it is always possible to obtain (7) with $k_3 = k_4 = 0$, which then reduces to the so-called control canonical form.

The characteristic equation of (7), which will be the starting point of our stability analysis, is given by

$$H(\lambda) = \lambda^2 + (a_1 + \bar{k}_1 e^{-\lambda})\lambda + (a_2 + \bar{k}_2 e^{-\lambda}) + \bar{k}_3 e^{-2\lambda}, \quad (8)$$

where

$$\begin{cases} \bar{k}_1 = k_1 + k_4 \\ \bar{k}_2 = k_2 + a_1 k_4 - a_2 k_3 \\ \bar{k}_3 = k_1 k_4 - k_2 k_3 \end{cases} . \quad (9)$$

When M is of rank 1, we have $\bar{k}_3 = 0$, and \bar{k}_1 and \bar{k}_2 can be assigned freely by an appropriate choice of k_1 and k_2 .

When the control term is of full rank, i.e. $\bar{k}_3 \neq 0$, there is a constraint on the possible values of the control parameters $\bar{k}_1, \bar{k}_2, \bar{k}_3$ in (8), meaning that the latter cannot always be considered as free parameters in the stabilizability analysis. This is the price we have to pay for the elimination of the redundancy in (7). Eliminating k_1 and k_2 from the first two equations of (9) and substituting in the last one leads to,

$$k_4^2 + a_2 k_3^2 - a_1 k_3^2 - a_1 k_3 k_4 + \bar{k}_1 k_4 - \bar{k}_2 k_3 - \bar{k}_3 = 0,$$

which can be written as,

$$Ax^2 + y^2 - B = 0$$

where

$$\begin{aligned} x &= k_3 + \frac{\bar{k}_1 a_1 / 2 - \bar{k}_2}{2(a_2 - a_1^2 / 4)}, & y &= k_4 - a_1 k_3 / 2 + \bar{k}_1 / 2, \\ A &= a_2 - a_1^2 / 4, & B &= \bar{k}_3 + \bar{k}_1^2 / 4 + \frac{(\bar{k}_1 a_1 / 2 - \bar{k}_2)^2}{4(a_2 - a_1^2 / 4)}. \end{aligned}$$

When $A \geq 0$ this equation can only have real solutions if $B \geq 0$ (meaning that for the given $\bar{k}_1, \bar{k}_2, \bar{k}_3$, corresponding values for k_1, k_2, k_3, k_4 exist). Hence the constraint on the control parameters in (8) is given by,

$$\bar{k}_3 \geq - \left(\bar{k}_1^2 / 4 + \frac{(\bar{k}_1 a_1 / 2 - \bar{k}_2)^2}{4(a_2 - a_1^2 / 4)} \right), \quad (10)$$

whenever $a_2 - \frac{a_1^2}{4} > 0$.

3.2 Class of stabilizable systems when $T = 1$

We want to determine the class of systems which are stabilizable with delayed state feedback. As follows from the canonical form (7), conditions on the system can be expressed in function of its parameters a_1 and a_2 . Note that $\lambda^2 + a_1\lambda + a_2 = 0$ is the characteristic polynomial of the (uncontrolled) system.

Define

$$c(a_1, a_2) = \min_M F(M), \quad (11)$$

where

$$F(M) = \sup \left\{ \Re(\lambda) : H(\lambda) = \det \left(\lambda I - A - M e^{-\lambda} \right) = 0 \right\}. \quad (12)$$

Then in the (a_1, a_2) -plane, stabilizable and unstabilizable systems are separated by curves on which $c(a_1, a_2) = 0$. In the rest of the paper we will refer to these curves as the stability boundary.

In Figure 3, the stability boundary is depicted. Before discussing its properties in Subsection 3.4, we first outline its computation.

An exhaustive way would consist of applying the continuous pole placement method, illustrated for the system (3)-(6) in the previous section, for a large number of values of the plant parameters (a_1, a_2) , which are chosen on a fine grid. The stability boundary then consists of values for which the method breaks down as the rightmost eigenvalues approach zero. However a more efficient calculation is possible by taking specific properties of the optimization problem (11) into account. This is now explained in detail for the case where M is of rank 1. Similar ideas apply to the case where M is of full rank.

Note first that the optimization problem (11) is not differentiable. Moreover it will turn out that, due to coinciding eigenvalues, discontinuities of derivatives of the objective function (12) precisely occur in the minimum and hence the latter cannot be calculated using the relations $\frac{dF}{dm_i} = 0$, where m_i is a component of M , since these define smooth extrema. On the other hand, note that in the example (3)-(6) the minimum is characterized by three coinciding rightmost eigenvalues. In the general case we have the following property, proven in the appendix:

Property 3.1 *When the function $F(M)$ with $M = BK^T$ in (12) is minimal, there are at least three eigenvalues with real part equal to $c(a_1, a_2)$.*

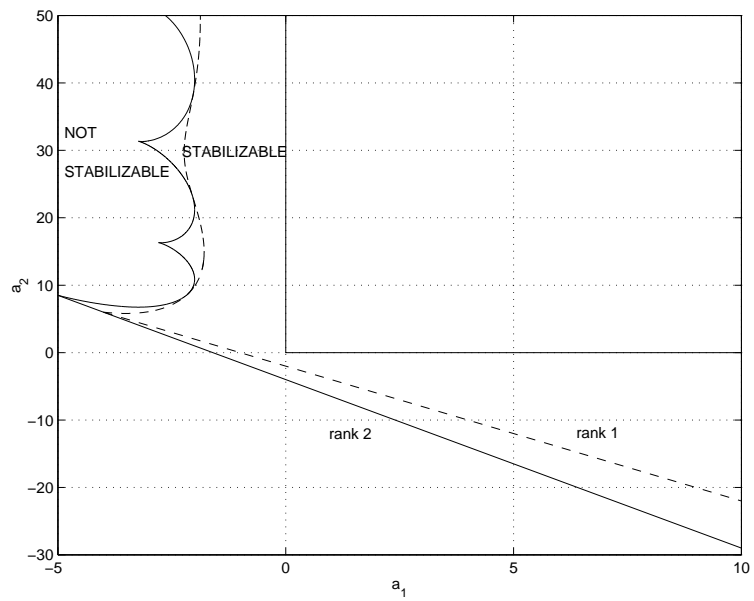


Figure 3: Stability boundary of (4)-(7) for $T = 1$ when M is rank 1 (dotted line) and M is rank 2 (full line). The characteristic equation of the open loop system is given by $\lambda^2 + a_1\lambda + a_2 = 0$.

As a consequence, the possible configurations of the rightmost eigenvalues at the global minimum of (12) can be reduced to the four basic situations shown in Table 1. From our numerical experiments it turned out that only situations I and II occur. Although we don't have a theoretical proof that situations I' and II' are not possible, we do have an intuitive explanation why these situations are at least less generic than situations I and II. In Table 1 the mathematical relations, which characterize the position of the rightmost eigenvalues, are also displayed. In cases I and II, these relations allow a direct computation of the minimal value c of (12) and the corresponding control parameters \bar{k}_1 and \bar{k}_2 when good starting values are available. In cases I' and II' however, there is an extra parameter and therefore the mathematical relations in Table 1 define curves through the point corresponding to the optimal parameter values. In such situations, a suitable small parameter change generically reduces¹ the value of c , meaning that the situation does not correspond to the global minimum, unless an extra condition is satisfied (e.g. a turning point). Apparently this extra condition is characterized by $\omega = 0$ for case I', which then reduces to case I, and by $\omega_2 = \omega_1$ for case II', which reduces to case II. These extra conditions are in some sense natural because situation II occurs for instance when the uncontrolled system is highly oscillatory, with ω approximating the natural frequency, whereas situation I occurs when it is highly damped, and in these cases an extra dominant 'frequency' in the controlled system is not expected.

Using the information contained in Table 1, the calculation of the stability boundary only requires to apply the continuous pole placement method for plant parameters chosen on a *coarse* grid. Indeed, suppose that we have applied the method for the plant parameters $(a_1^{(i)}, a_2^{(i)})$, $i = 1, 2$, leading to $c(a_1^{(1)}, a_2^{(1)}) > 0$ and $c(a_1^{(2)}, a_2^{(2)}) < 0$. Then these two pairs are separated by the stability boundary. Moreover, when they are close together, information is provided about the type of the minimum (I or II) to be expected on the stability boundary in that neighbourhood. This allows to compute points on the stability boundary directly using the mathematical relations displayed in Table 2. Since compared to Table 1, at one hand the extra condition $c = 0$ is required on the stability boundary but on the other hand the parameters a_1 and a_2 are freed, these mathematical relations define a branch which can be numerically continued in an efficient way. Good starting values are ob-

¹This is not only the case for the solution of the equations in Table 1 but also for the eigenvalues of the corresponding DDE, because with an arbitrarily small parameter change, the other eigenvalues (i.e. which are not rightmost) can not influence the right spectral upper bound, $\sup \Re(\lambda)$. This follows from continuity properties of the spectrum w.r.t. parameter changes. For more details, see the appendix of [8].

Poss.	Rightmost eigenvalues (multiplicity)	Equations	Unknowns
I	c ($3f$)	$\begin{cases} H(c) = 0 \\ H^{(1)}(c) = 0 \\ H^{(2)}(c) = 0 \end{cases}$	c, \bar{k}_1, \bar{k}_2
(I')	c $c \pm j\omega$	$\begin{cases} H(c) = 0 \\ \Re(H(c + j\omega)) = 0 \\ \Im(H(c + j\omega)) = 0 \end{cases}$	$c, \omega, \bar{k}_1, \bar{k}_2$
II	$c \pm j\omega$ ($2f$)	$\begin{cases} \Re(H(c + j\omega)) = 0 \\ \Im(H(c + j\omega)) = 0 \\ \Re(H^{(1)}(c + j\omega)) = 0 \\ \Im(H^{(1)}(c + j\omega)) = 0 \end{cases}$	$c, \omega, \bar{k}_1, \bar{k}_2$
(II')	$c \pm j\omega_1$ $c \pm j\omega_2$	$\begin{cases} \Re(H(c + j\omega_1)) = 0 \\ \Im(H(c + j\omega_1)) = 0 \\ \Re(H(c + j\omega_2)) = 0 \\ \Im(H(c + j\omega_2)) = 0 \end{cases}$	$c, \omega_1, \omega_2, \bar{k}_1, \bar{k}_2$

Table 1: According to Property 3.1, four configurations of the rightmost eigenvalues are possible in the global minimum of (12), when M is of rank 1. However only situation I and II occur. In the second column the mathematical relation, which characterize each configuration, are displayed. $H^{(i)}$ refers to the i -th derivative of H w.r.t. λ .

tained by the results of the continuous pole placement method for the plant parameters $(a_1^{(i)}, a_2^{(i)})$ and the emanating branch coincides at least locally with the stability boundary.

According to Table 2, the components of the stability boundary are displayed in Figure 4. The frequency ω on branch II approximates the natural frequency of the open loop system and tends to zero along the branch when approaching the intersection with branch I.

When the control term is of full rank, there are three control parameters $\bar{k}_1, \bar{k}_2, \bar{k}_3$ in (8). The configurations of the rightmost eigenvalues on the stability boundary are analogous to the previous case but, since there is an extra control parameter, one extra condition on the right most eigenvalues needs to be fulfilled, see Table 2. Four cases can be distinguished and accordingly the stability boundary can be decomposed in four components, see Figure 4. The presence of an extra control parameter leads to 4 coinciding real eigenvalues on branch III and 2 coinciding pairs of complex conjugate eigenvalues and 1 real eigenvalue on branch IV. The calculation of branches V and VI deserves further attention. Consider therefore Figure 5. Point A lies on branch II, hence $\bar{k}_3 = 0$ and its parameters $\bar{k}_1, \bar{k}_2, \omega, a_1, a_2$ satisfy

$$\begin{cases} \Re(H(j\omega)) = 0 \\ \Im(H(j\omega)) = 0 \\ \Re(H^{(1)}(j\omega)) = 0 \\ \Im(H^{(1)}(j\omega)) = 0 \end{cases} \quad (13)$$

We now free parameter \bar{k}_3 , and while keeping a_2 constant, we continue the solution of (13) as a function of a_1 . The turning point B, where a minimum of a_1 is reached, defines a point of branch V. In such a bifurcation point,

$$\det \left(J_{\bar{k}_1, \bar{k}_2, \bar{k}_3, \omega}(H, H^{(1)}) \right) = 0 \quad (14)$$

is satisfied [11], where $J_{\bar{k}_1, \bar{k}_2, \bar{k}_3, \omega}(H, H^{(1)})$ is the Jacobian matrix of (13) as a function of parameters $\bar{k}_1, \bar{k}_2, \bar{k}_3, \omega$. By computing a branch of turning point in the (a_1, a_2) -plane, i.e. by continuing² the solution of (13)-(14), branch V is obtained.

Notice that constraint (10) forms a lower bound on \bar{k}_3 . When $32.4 \leq a_2 \leq 34.8$ and a continuation as in Figure 5 is performed, the constraint on \bar{k}_3 becomes active before the turning point is reached and determines the

²Since (14) is intractable from a numerical point of view, the equivalent system $\begin{cases} J_{\bar{k}_1, \bar{k}_2, \bar{k}_3, \omega}(H, H^{(1)})X = 0 \\ X^T X = 1 \end{cases}$ is used in our numerical calculations.

Branch	RM eig. (multiplicity)	Equations	Unknowns (\rightarrow Analytic solution)
I	0 (3f)	$\begin{cases} H(0) = 0 \\ H^{(1)}(0) = 0 \\ H^{(2)}(0) = 0 \end{cases}$	$a_1, a_2, \bar{k}_1, \bar{k}_2$ $\rightarrow a_2 = -2a_1 - 2$
II	$\pm j\omega$ (2f)	$\begin{cases} H(j\omega) = 0 \\ H^{(1)}(j\omega) = 0 \end{cases}$	$a_1, a_2, \bar{k}_1, \bar{k}_2, \omega$
III	0 (4f)	$\begin{cases} H(0) = 0 \\ H^{(1)}(0) = 0 \\ H^{(2)}(0) = 0 \\ H^{(3)}(0) = 0 \end{cases}$	$a_1, a_2, \bar{k}_1, \bar{k}_2, \bar{k}_3$ $\rightarrow a_2 = -2.5a_1 - 4$
IV	0 $\pm j\omega$ (2f)	$\begin{cases} H(0) = 0 \\ H(j\omega) = 0 \\ H^{(1)}(j\omega) = 0 \end{cases}$	$a_1, a_2, \bar{k}_1, \bar{k}_2, \bar{k}_3, \omega$
V	$\pm j\omega$ (2f)	$\begin{cases} H(j\omega) = 0 \\ H^{(1)}(j\omega) = 0 \\ \det(J_{\bar{k}_1, \bar{k}_2, \bar{k}_3, \omega}(H, H^{(1)})) = 0 \end{cases}$	$a_1, a_2, \bar{k}_1, \bar{k}_2, \bar{k}_3, \omega$
VI	$\pm j\omega$ (2f)	$\begin{cases} H(j\omega) = 0 \\ H^{(1)}(j\omega) = 0 \\ \bar{k}_3 = -\left(\bar{k}_1^2/4 + \frac{(\bar{k}_1 a_1/2 - \bar{k}_2)^2}{4(a_2 - a_1^2/4)}\right) \end{cases}$	$a_1, a_2, \bar{k}_1, \bar{k}_2, \bar{k}_3, \omega$

Table 2: Positions of the rightmost eigenvalues on the stability boundary in the 2D case and determining systems. $H^{(i)}$ refers to the i -th derivative of H w.r.t. λ . Situations I and II occur when M is rank 1, situations III, IV, V and VI when M is rank 2. The corresponding mathematical relations define branches, of which the stability boundary is composed.

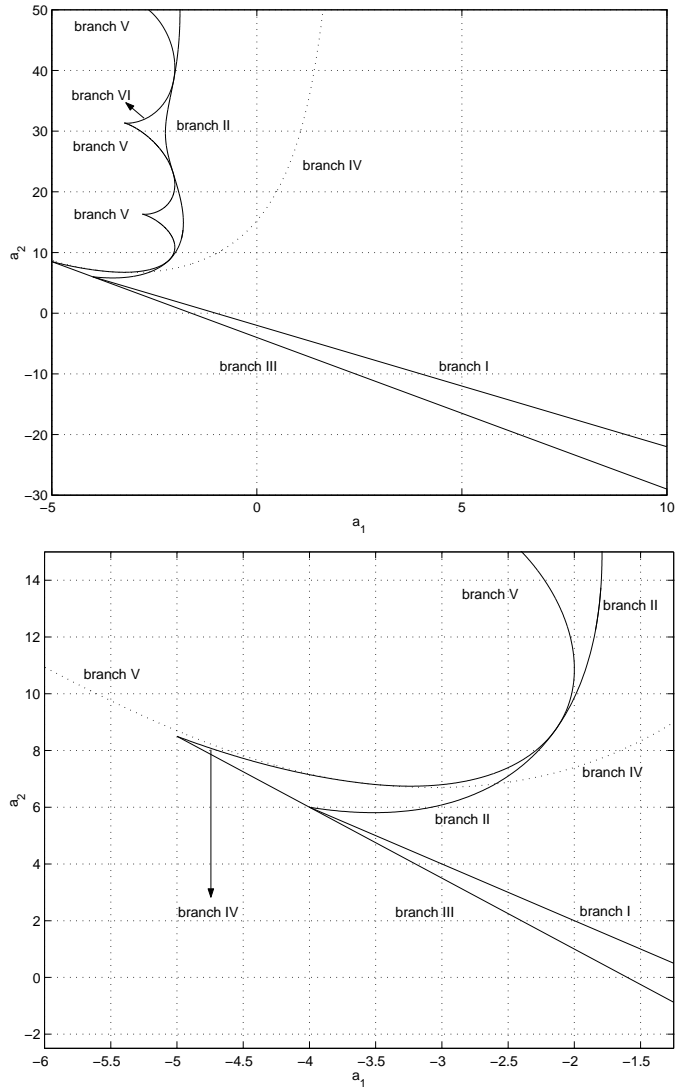


Figure 4: Components of the stability boundary (above) and detail (below). The different branches refer to Table 2.

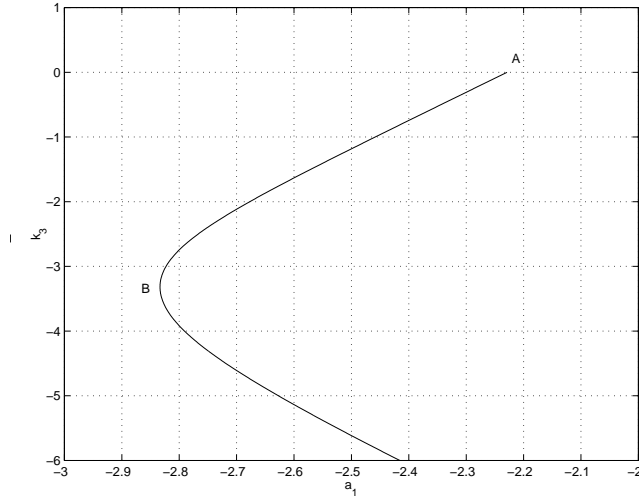


Figure 5: When fixing a_2 and continuing the solution of (13) from point A on branch II as a function of parameter a_1 , a turning point B occurs. Branch V is composed of such turning points. In point A we have $(a_1, a_2) = (-2.223, 30)$.

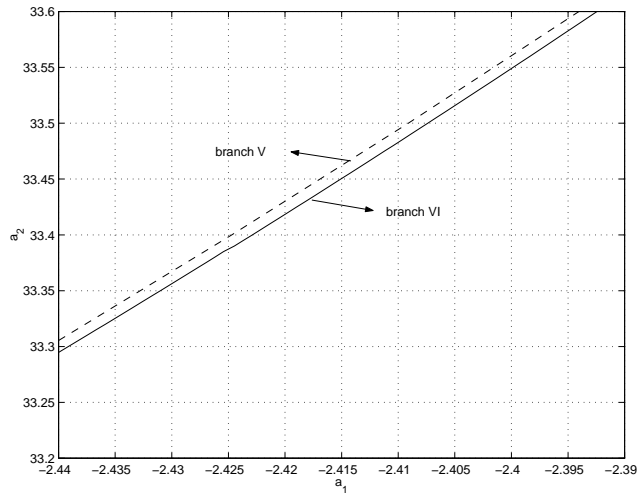


Figure 6: For $32.4 \leq a_2 \leq 34.8$, the stability boundary is not formed by branch V (dashed line), but by branch VI (full line). On branch VI, (10) is an equality constraint.

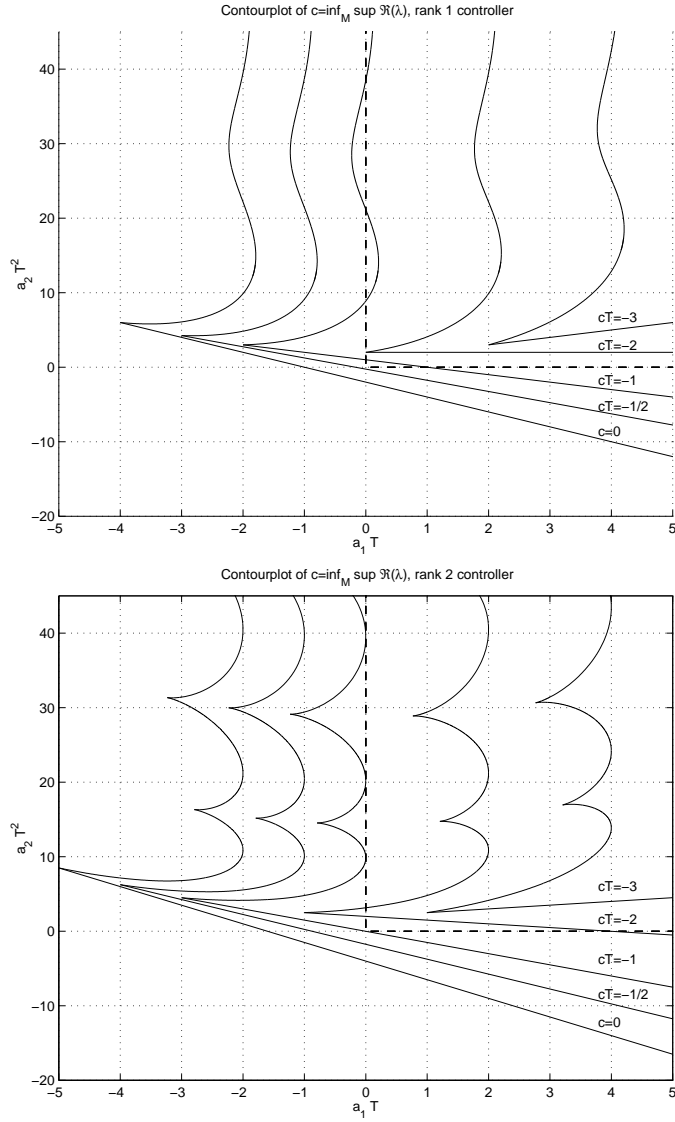


Figure 7: Contour lines of $c(a_1, a_2, T)$ as a function of the system parameters a_1 , a_2 and T , where M is of rank 1 (above) and of rank 2 (below). These contour lines correspond to the maximal achievable exponential decay rate of the solutions of (3) and (4) in the 2D-case. The stability boundary consists of the contour line $c = 0$.

minimal value of a_1 . In this case the stability boundary is determined by equations (13) and

$$\bar{k}_3 = - \left(\bar{k}_1^2/4 + \frac{(\bar{k}_1 a_1/2 - \bar{k}_2)^2}{4(a_2 - a_1^2/4)} \right),$$

which expresses that constraint (10) is active. This part of the stability boundary coincides with branch VI, see Figure 6.

3.3 Class of stabilizable system: the general case

We now consider the computation of the stability boundary of (4) when the delay $T \neq 1$. Furthermore we show how contour lines of $c(a_1, a_2, T)$, defined by

$$c(a_1, a_2, T) = \min_M \left\{ \sup \left\{ \Re(\lambda) : \det \left(\lambda I - A - M e^{-\lambda T} \right) = 0 \right\} \right\},$$

can be calculated. Consider therefore

$$\det \left(\lambda I - A - M e^{-\lambda T} \right) = 0, \quad (15)$$

the characteristic equation of (4). With the substitution

$$\bar{\lambda} = T(\lambda - \alpha/T),$$

(15) is written as,

$$\det \left(\bar{\lambda} I - (TA - \alpha I) - TM e^{\alpha} e^{-\bar{\lambda}} \right) = 0,$$

which is the characteristic equation of

$$\dot{x} = \bar{A}x + \bar{M}x(t-1), \quad \bar{A} = TA - \alpha I, \quad \bar{M} = TM e^{\alpha}. \quad (16)$$

The stability boundary of the system (16), which satisfies the assumptions of the previous subsections, corresponds to the contour line $c(a_1, a_2, T)T = \alpha$ and is expressed in function of the parameters of \bar{A} . Note that, as follows from the definition of \bar{A} , contour lines can be expressed in the normalized coordinates $a_1 T$ and $a_2 T^2$, where $\lambda_2 + a_1 \lambda + a_2 = 0$ is the characteristic equation of the open loop system. The contour line $c = 0$ forms the stability boundary of the original system (4). In Figure 7 contour lines of $c(a_1, a_2, T)$ are shown as a function of the parameters a_1, a_2 and T . These lines correspond to the maximal achievable exponential decay rate of the solutions of (3) and (4).

3.4 Discussion

We now summarize some interesting properties of delayed state feedback by means of Figure 7.

The uncontrolled system is only asymptotically stable when $a_1 > 0$ and $a_2 > 0$. With delayed state feedback, the class of stabilizable systems is determined by the stability boundary. This class becomes larger and grows unbounded in all directions as the delay is reduced. Contrary to the ODE-case, where the whole spectrum can be controlled with rank 1 feedback, the class of stabilizable systems is considerably larger with rank 2 feedback in the time-delay case, a consequence of the infinite-dimensional nature of DDEs.

Fix the plant parameters (a_1, a_2) and consider its stabilizability properties as a function of the delay. In Figure 7 a change of the delay T corresponds to a movement of the normalized plant parameters $(\hat{a}_1, \hat{a}_2) = (a_1 T, a_2 T^2)$ on a (half) parabola. When the plant has an eigenvalue in the open right half plane, i.e. either $a_1 < 0$ or $a_2 < 0$, this parabola always intersects the stability boundary, hence when the uncontrolled system is (exponentially) unstable, it cannot be stabilized for large values of the time-delay, which is expected from Theorems 1 and 2 in [8]. On the other hand, when the rightmost eigenvalue of the open loop system lies on the imaginary axis, stabilization is always possible, whatever the value of the time-delay. For large T , the corresponding control law has a low-gain character. When the delay is brought to zero, we have $(\hat{a}_1, \hat{a}_2) \rightarrow (0, 0)$ and consequently $cT \rightarrow -\hat{c}$, with $\hat{c} > 0$ constant. Hence for small T , the maximal achievable exponential decay rate is proportional to $1/T$. It is easy to verify that this result also holds when the dimension of the plant is larger than two. Note that as $T \rightarrow 0+$, $c \rightarrow -\infty$, which corresponds to the ODE-case where the eigenvalues can be assigned arbitrarily.

When T is fixed and $a_2 \rightarrow \infty$, the stability boundary doesn't asymptotically approach the a_2 -axis, although the natural frequencies of the corresponding uncontrolled systems tend to infinity. For a class of unstable systems with highly oscillatory behaviour, stabilization with delayed feedback is intuitively possible because tuning of the parameter M in (4) allows to give the feedback signal Me the right phase-shift, thereby compensating (mod 2π) the phase-shift introduced by the delay. But this also implies that the larger a_2 , the more sensitive is the achieved stability w.r.t. changes in system parameters and in particular the delay.

4 Applications

In this section we outline some applications where problems of the form (3)-(4) arise, based on [8, 9]. Thereby we explain how the limitations of delayed state feedback, discussed in the previous section, affect these applications.

With the controller (2), full state feedback is used in (3) to stabilize the system (1). Assume now that not the state x , but only an output $y = C^T x \in \mathbb{R}$, is available for measurement, with (C, A) observable. In that case, the plant can be equivalently described by the transfer function

$$G_P(s) = G(s)e^{-sT}, \quad (17)$$

with $G(s) = C^T(sI - A)^{-1}B$, and any system of the form

$$\dot{x} = Ax + Bu(t - T_1), \quad y = C^T x(t - T_2), \quad T_1 + T_2 = T, \quad (18)$$

is a realization of (17). In order to apply delayed state feedback, we first construct an observer for (18),

$$\dot{\hat{x}} = A\hat{x} + Bu(t - T_1) + L(C^T \hat{x}(t - T_2) - y), \quad (19)$$

with $L \in \mathbb{R}^{n \times 1}$ the observer gain, and apply the feedback $u = K^T \hat{x}(t)$. With $e = x - \hat{x}$ the observer error, we obtain

$$\begin{cases} \dot{x} = Ax + BK^T x(t - T_1) - BK^T e(t - T_1) \\ \dot{e} = Ae + LC^T e(t - T_2) \end{cases}. \quad (20)$$

Since the system (20) is triangular, the separation principle is valid and the closed loop eigenvalues consist of the solutions of

$$\det(\lambda I - A - BK^T e^{-\lambda T_1}) = 0,$$

the controller eigenvalues, and of

$$\det(\lambda I - A - LC^T e^{-\lambda T_2}) = \det(\lambda I - A^T - CL^T e^{-\lambda T_2}) = 0,$$

the observer eigenvalues respectively. Hence by solving two problems of the form (3), with model parameters (A, B, T_1) and (A^T, C, T_2) , we can try to achieve stabilization.

In the construction of the realization (18), we are free to distribute the delay over input and output. This additional degree of freedom can be used to obtain better performance of plant and observer, and also allows to extend the class of stabilizable systems with delayed state feedback. In

the 2D-case, this follows from Figure 7a where, among other things, the stability boundary is depicted, expressed in the normalized plant parameters (a_1T, a_2T^2) . When the time-delay T is equally spread over input and output in (18)-(19), a system with parameters (a_1, a_2) (and open loop poles $\lambda_{1,2}$) is stabilizable with the observer based controller iff the system $(a_1/2, a_2/4)$ (with open loop poles $\lambda_{1,2}/2$) is stabilizable with full state feedback. Hence for very unstable systems or for large delay values, the construction of an observer is beneficial, even if the full state is available for measurement.

Note that when $T_1 = 0$ and $T_2 = T$ in (19), $y_p = C^T \hat{x}$ is a prediction of the output of (17) over one delay interval, and can be used as a feedback signal to any output feedback controller designed for the corresponding undelayed system, since the delay is compensated by the prediction. In [9], this idea is worked out, leading to a modification of the classical Smith Predictor [10, 12], which is also applicable to the class of unstable systems, characterized by the stabilizability of the observer dynamics (second equation of (20)), i.e. a problem of the form (3). As shown in the previous sections, better stability properties can be obtained when the components of M in (4) can be chosen independently. The limitations of a rank 1 control term, as in equation (3), can be avoided by generating y_p with a cascade of 2 observers, as proposed in [9], the first based on a model with an input delay and the other based on a model with an output delay, and described by,

$$\begin{cases} \dot{\hat{x}}_1 = A\hat{x}_1 + Bu(t-T) + L(C\hat{x}_1 - y), \\ \dot{\hat{x}}_2 = A\hat{x}_2 + Bu(t) + M(\hat{x}_2(t-T) - \hat{x}_1), \quad y_p = C\hat{x}_2, \end{cases} \quad (21)$$

see Figure 8. With $e_1 = \hat{x}_1 - x(t-T)$ and $e_2 = \hat{x}_2 - x$, where x is the state of an output delay representation of (17), the observer dynamics are governed by

$$\begin{cases} \dot{e}_1 = (A + LC)e_1, \\ \dot{e}_2 = Ae_2 + Me_2(t-T) - Me_1. \end{cases} \quad (22)$$

The observer eigenvalues now consist of the eigenvalues of

$$\dot{e}_1 = (A + LC^T)e_1, \quad L \in \mathbb{R}^{n \times 1},$$

which can be assigned arbitrarily, and of

$$\dot{e}_2 = Ae_2 + Me_2(t-T), \quad M \in \mathbb{R}^{n \times n}, \quad (23)$$

where the components of M can be chosen independently.

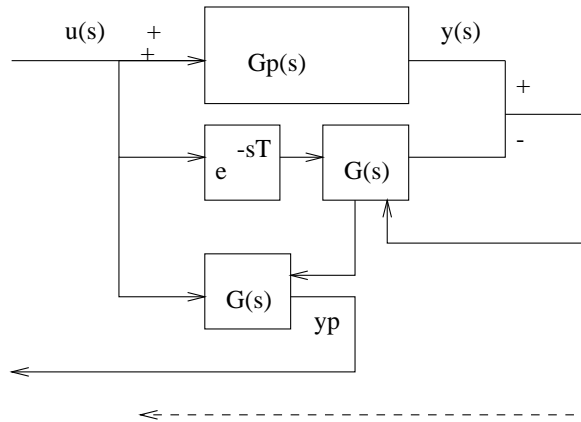


Figure 8: Cascade of two observers generating a prediction y_p of the output of (17).

Acknowledgements

This paper presents research results of the Belgian programme on Interuniversity Poles of Attraction, initiated by the Belgian State, Prime Minister's Office for Science, Technology and Culture (IUAP P4/02). The scientific responsibility rests with its author.

References

- [1] D. Brethé and J.J. Loiseau. An effective algorithm for finite spectrum assignment of single-input systems with delays. *Mathematics and Computers in Simulation*, 45:339–348, 1998.
- [2] M. Cardelli, V. Van Assche, and L.L. Loiseau. About numerical approximations of a stabilizing distributed delay control law. In *Proceedings of MTNS 2000*, Perpignan, France, 2000.
- [3] K. Engelborghs. DDE-biftool: a matlab package for bifurcation analysis of delay differential equations. TW Report 305, Department of Computer Science, Katholieke Universiteit Leuven, Belgium, March 2000.
- [4] K. Engelborghs, M. Dambrine, and D. Roose. Limitations of a class of stabilization methods for delay equations. *IEEE Transactions on Automatic Control*, 46(2):336–339, 2001.

- [5] K. Engelborghs and D. Roose. Numerical computation of stability and detection of hopf bifurcations of steady state solutions of delay differential equations. *Advances in Computational Mathematics*, 10(3-4):271–289, 1999.
- [6] J.K. Hale and S.M. Verduyn Lunel. *Introduction to functional differential equations*, volume 99 of *Applied mathematical sciences*. Springer Verlag, 1993.
- [7] V.B. Kolmanovskii and A. Myshkis. *Introduction to the theory and application of functional differential equations*, volume 463 of *Mathematics and its applications*. Kluwer Academic Publishers, 1999.
- [8] W. Michiels, K. Engelborghs, P. Vansevenant, and D. Roose. Continuous pole placement method for delay equations. In A.M. Perdon, editor, *Proceedings of the 2nd Workshop on Linear Time Delay Systems*, pages 129–134, 2000. Extended version submitted to *Automatica*.
- [9] W. Michiels and D. Roose. Time-delay compensation in unstable plants using delayed state feedback. In *Proceedings of the 40th IEEE Conference on Decision and Control*, 2001. Submitted.
- [10] Z.J. Palmor. *The Control Handbook*, chapter 10, pages 224–237. CRC and IEEE Press, New York, 1996.
- [11] R. Seydel. *Practical bifurcation and stability analysis: from equilibrium to chaos*, volume 5 of *Interdisciplinary applied mathematics*. Springer New-York, 1994.
- [12] O.J. Smith. Closer control of loops with dead time. *Chem.Eng.Prog.*, 53:217–219, 1957.
- [13] Q.G. Wang, T.H. Lee, and K.K. Tan. *Finite Spectrum Assignment for Time-Delay Systems*, volume 239 of *Lecture Notes in Control and Information Sciences*. Springer Verlag, 1998.

A Proof of Property 3.1

Note first from the linearity of (8) w.r.t. the control parameters that two eigenvalues can always be placed arbitrarily in the complex plane. When

we require $H(\lambda_1) = H(\lambda_2) = 0$ with $\lambda_1 \neq \lambda_2$, the control parameters can be calculated from

$$\begin{bmatrix} \lambda_1 & 1 \\ \lambda_2 & 1 \end{bmatrix} \begin{bmatrix} \bar{k}_1 \\ \bar{k}_2 \end{bmatrix} = \begin{bmatrix} -\lambda_1^2 e^{\lambda_1} - a_1 e^{\lambda_1} \lambda_1 - a_2 e^{\lambda_1} \\ -\lambda_2^2 e^{\lambda_2} - a_1 e^{\lambda_2} \lambda_2 - a_2 e^{\lambda_2} \end{bmatrix}, \quad (24)$$

and when we require $H(\lambda_0) = H^{(1)}(\lambda_0) = 0$ (i.e. a double eigenvalue at λ_0), we have

$$\begin{bmatrix} \lambda_0 - 1 & 1 \\ \lambda_0 & 1 \end{bmatrix} \begin{bmatrix} \bar{k}_1 \\ \bar{k}_2 \end{bmatrix} = \begin{bmatrix} 2\lambda_0 e^{\lambda_0} + a_1 e^{\lambda_0} \\ -\lambda_0^2 e^{\lambda_0} - a_1 e^{\lambda_0} \lambda_0 - a_2 e^{\lambda_0} \end{bmatrix}. \quad (25)$$

Assume now that (12) is minimal for $(\bar{k}_1^m, \bar{k}_2^m)$ and that there are less than three eigenvalues with real part equal to c . Denote the two rightmost eigenvalues by λ_1, λ_2 and for any $\epsilon > 0$, calculate from (24) or (25) the control parameters $(\bar{k}_1(\epsilon), \bar{k}_2(\epsilon))$ which result in two eigenvalues at $\lambda_1 - \epsilon$ and $\lambda_2 - \epsilon$. From the continuity of (24)-(25) we have $(\bar{k}_1(\epsilon), \bar{k}_2(\epsilon)) \rightarrow (\bar{k}_1^m, \bar{k}_2^m)$ as $\epsilon \rightarrow 0+$. Hence with an arbitrarily small change in the controller parameters the two rightmost eigenvalues can be moved to the left, while the other eigenvalues can not become dominant, as follows from the ideas spelled out in the proof of Theorem 8 of [8]. This contradicts the assumption of a minimum of (12). \square